

Influence of sulfur doping on the molecular fluorophore and synergistic effect for citric acid carbon dots

Guohua Cao(曹国华), Zhifei Wei(魏志飞), Yuehong Yin(殷月红), Lige Fu(付丽歌), Yukun Liu(刘玉坤), Shengli Qiu(邱胜利), and Baoqing Zhang(张宝庆)

Citation: Chin. Phys. B, 2021, 30 (**9**): 097802. DOI: 10.1088/1674-1056/abfbd5
Journal homepage: http://cpb.iphy.ac.cn; http://iopscience.iop.org/cpb

What follows is a list of articles you may be interested in

A review of experimental advances in twisted graphene moirè superlattice

Yanbang Chu(褚衍邦), Le Liu(刘乐), Yalong Yuan(袁亚龙), Cheng Shen(沈成), Rong Yang(杨蓉), Dongxia Shi(时东霞), Wei Yang(杨威), and Guangyu Zhang(张广宇)

Chin. Phys. B, 2020, 29 (**12**): 128104. DOI: 10.1088/1674-1056/abb221

A new sulfur-doped source and synergistic effect with nitrogen for carbon dots produced from glucose

Lige Fu(付丽歌), Yuehong Yin(殷月红), Guohua Cao(曹国华), Pingping Wu(武苹苹), Jian Wang(汪舰), Lingling Yan(闫玲玲), Baoqing Zhang(张宝庆), Ming Li(李明)

Chin. Phys. B, 2019, 28 (**12**): 128102. DOI: 10.1088/1674-1056/ab5213

Density functional calculations of efficient H_2 separation from impurity gases (H_2, N_2, H_2O, CO, Cl_2, and CH_4) via bilayer g-C_3N_4 membrane

Yuan Guo(郭源), Chunmei Tang(唐春梅), Xinbo Wang(王鑫波), Cheng Wang(王成), Ling Fu(付玲)

Chin. Phys. B, 2019, 28 (**4**): 048102. DOI: 10.1088/1674-1056/28/4/048102

Modulated thermal transport for flexural and in-plane phonons in double-stub graphene nanoribbons

Chang-Ning Pan(潘长宁), Meng-Qiu Long(龙孟秋), Jun He(何军)

Chin. Phys. B, 2018, 27 (**8**): 088101. DOI: 10.1088/1674-1056/27/8/088101

Bright blue photoluminescence from a mixed tin and manganese oxide xerogel prepared via sol–hydrothermal–gel process

Xiang Xia, Cheng Xiao-Feng, He Shao-Bo, Yuan Xiao-Dong, Zheng Wan-Guo, Li Zhi-Jie, Liu Chun-Ming, Zhou Wei-Lie, Zu Xiao-Tao

Chin. Phys. B, 2011, 20 (**12**): 127801. DOI: 10.1088/1674-1056/20/12/127801

Influence of sulfur doping on the molecular fluorophore and synergistic effect for citric acid carbon dots*

Guohua Cao(曹国华)[1], Zhifei Wei(魏志飞)[2], Yuehong Yin(殷月红)[1,†], Lige Fu(付丽歌)[1], Yukun Liu(刘玉坤)[2], Shengli Qiu(邱胜利)[2], and Baoqing Zhang(张宝庆)[2,‡]

[1] *School of Physics and Electronic Information Engineering, Henan Polytechnic University, Jiaozuo* 454000, *China*
[2] *School of Materials Science and Engineering, Henan Polytechnic University, Jiaozuo* 454000, *China*

(Received 1 March 2021; revised manuscript received 17 April 2021; accepted manuscript online 27 April 2021)

In citric acid-based carbon dots, molecular fluorophore contributes greatly to the fluorescence emission. In this paper, the nitrogen and sulfur co-doped carbon dots (N,S-CDs) were prepared, and an independent sulfur source is selected to achieve the doping controllability. The influence of sulfur doping on the molecular fluorophore was systematically studied. The introduction of sulfur atoms may promote the formation of molecular fluorophore due to the increased nitrogen content in CDs. The addition surface states containing sulfur were produced, and S element exists as $-SO_3$, and $-SO_4$ groups. Appreciate ratio of nitrogen and sulfur sources can improve the fluorescence emission. The photoluminescence quantum yields (PLQY) is increased from 56.4% of the single N-doping CDs to 63.4% of double-doping CDs, which ascribes to the synergistic effect of molecular fluorophores and surface states. The sensitivity of fluorescence to pH response and various metal ions was also explored.

Keywords: carbon dots, citric acid, sodium sulfite, molecular fluorophore, synergistic effect

PACS: 78.30.Na, 81.05.U−, 73.63.Kv **DOI:** 10.1088/1674-1056/abfbd5

1. Introduction

Fluorescent carbon dots (CDs) are prospective materials owing to their outstanding optical properties, tunable surface functional groups, good bio-compatibility, and low cost.[1–5] Until now, various CDs have been prepared from molecular precursors, multiwalled carbon nanotubes, activated carbon, and natural plants via a variety of methods, such as hydrothermal routes, laser ablation, microwave routes, chemical oxidation, and plasma method.[6–9] Because the performance of CDs is not enough to meet the requirements of practical application, a great deal of effort has been invested in the development of CDs. Doping CDs with heteroatom is confirmed to be an effective pathway to improve their optical properties.[10–12] Among the various doping elements, nitrogen is often used to promote the unique properties of CDs due to their close atomic size to the carbon, and much progress has been made.[13,14] Moreover, double-doped CDs are also explored in order to tune the intrinsic properties towards appropriate applications.[15,16] Li *et al.*[17] reported a double doping strategy of N/Mg-doped CDs with citric acid (CA), $Mg(OH)_2$, and ethylenediamine (EDA) as sources, and the photoluminescence quantum yields (PLQY) is significantly enhanced.

Citric acid CDs and citrate-based fluorescent materials have received much interest due to their intrinsic advantages, such as tunable emission, low toxicity, high quantum yields, and simple synthesis procedures.[18,19] Among the most common synthesis methods toward CDs using CA and amine, molecular fluorophores have been expected to form and contribute to their high PLQY.[20–22] For example, the CDs prepared by CA and EDA have formed the fluorescent molecule, 5-oxo-1,2,3,5-tetrahydroimidazo(1,2-a) pyridine-7-carboxylic acid (IPCA). The CDs derived from CA and hexamethylenetetramine as sources produced a parallel formation of the fluorophores.[23] The formation and properties of molecular fluorophores have been influenced by the type of amine, reaction temperature, and so on.[24,25] Importantly, the double doping also has a great influence on the fluorescence properties of CA CDs. It is recommended that nitrogen and sulfur co-doped CDs (N,S-CDs) is a practicable method to increase the optical properties of CA CDs, and the QY of N,S-CDs is higher than that of single N-doped CDs (N-CDs).[26] Wu *et al.*[27] demonstrated that N,S-CDs synthesized with CA and cysteine show high PLQY of 69%. They attributed these results to the enhancement of nitrogen-luminescent centers due to the introduction of S atoms. Although much progress has been made in the research of CA CDs, there are relatively few studies on the characteristic of the molecular fluorophores in double doping CA CDs, especially the effects from the sulfur doping.

For N,S-CDs, nitrogen and sulfur elements are mostly

*Project supported by the National Natural Science Foundation of China (Grant No. 51571085) and the Key Scientific Research Projects of Colleges and Universities in Henan Province, China (Grant No. 20A430015).

†Corresponding author. E-mail: yuehongyin@126.com
‡Corresponding author. E-mail: bqzhang@hpu.edu.cn

© 2021 Chinese Physical Society and IOP Publishing Ltd

derived from the same organic source, such as cysteine,[27] thiourea,[28] and so on. In order to elucidate the effect of heteroatom doping on molecular fluorophore, it is necessary to introduce an independent doping source. Compared with organic materials, inorganic sulfur source possesses simple structure, strong controllability, better water solubility, and wide application range. In the present work, sodium sulfite (Na_2SO_3) was selected as sulfur source, and N,S co-doped CA CDs were prepared via the hydrothermal route. We compare the structure and optical properties of N-CDs and N,S-CDs, and discuss the influence of S doping on the molecular fluorophores. Furthermore, the pH response and the sensitivity for the detection of metal ions using N,S-CDs was investigated and the involved mechanism was discussed.

2. Experimental procedures

2.1. Synthesis of CDs

The CDs were prepared via hydrothermal method with CA as carbon source, EDA as nitrogen source and Na_2SO_3 as sulfur source. CA (AR, 99.5%), EDA (AR, 99%), and Na_2SO_3 (AR, 98%) were obtained from Aladdin Chemistry Co., Ltd. All reagents were directly used without further purification. Sodium hydroxide (NaOH, AR, 96%) was used to tune the pH of the solution.

The typical hydrothermal procedure was conducted to prepare CA-based CDs. For the single N-doped CDs, the molar ratio of CA:EDA was 1:2. 1-mmol CA (0.1921 g) and 2-mmol EDA (134 μL) were dispersed in 10-mL distilled water, and then mixture obtained was put in a Teflon-lined autoclave. The hydrothermal process was adopted at 140 °C for a period of 5 hours. After reaction, on cooling to room temperature, the products were then further filtered, dialyzed and dried to obtain resulting N-CDs. For N,S-CDs, the similar synthetic procedure was performed. The N,S-CDs sample with CA:EDA:Na_2SO_3 at 1:2:1 was chosen for comparison. To further study the effect of doping source, the various N,S-CDs were synthesized by changing the molar ratio of EDA and Na_2SO_3. The molar ratios of CA: EDA: Na_2SO_3 were 1:1:1, 1:2:1, 1:3:1, 1:1:2, 1:1:3, and 1:2:2, respectively.

2.2. PH response and fluorescence detection

For pH response measurement, sodium hydroxide with 2% (wt%) and sulfuric acid were used to realize the solutions with different pH values. The pH values were selected as 3, 5, 7, 9, 11 and 13. The detection of metal ions was carried out in 1-mL N,S-CDs solution (0.1 mg/mL). Metal ions (Al^{3+}, K^{+}, $Cu^{2}+$, Mg^{2+}, Cd^{2+}, Zn^{2+}, Ca^{2+}, and Fe^{3+}) at the same concentration of 1 mM was injected separately in the N,S-CDs solution. The sensitive detection of Fe^{3+} was executed in 1-mL solution with different concentrations of 0, 20, 60, 100, 160, 220, 300, 400, 500, and 600 μM, respectively. The 1-mL N,S-CDs solution was added and mixed thoroughly before characterization.

2.3. Characterization

The structure of samples was measured by the x-ray diffraction (XRD, Shimadzu XRD-6000). The morphology was observed on the transmission electron microscopy (TEM) and high-resolution transmission electron microscopy (HRTEM, FEI Talos F200X). Fourier transform infrared spectra (FTIR) of the CDs were obtained on Nicolet 460 FT-IR spectrometer (Thermo Nicolet, USA). The chemical structure was measured using x-ray photoelectron spectra (XPS, Escalab 250XI. The absorption spectra were examined with an UV-visible-infrared spectrophotometer (UV-3600, Shimadzu). The PL spectra and the lifetime were recorded using Fluorolog-3 (Horbia Scientific). The photoluminescence quantum yield was analyzed by Horiba Jobin Yvon fluororomax-4 spectro-fluorometer.

3. Results and discussion

3.1. Structural characterization

Figure 1(a) displays the XRD patterns of N-CDs and N,S-CDs. For the two CDs, there is a broad peak to be observed, while the peak centered is about 18.42° for N-CDs and 22.32° for N,S-CDs. The diffraction angle and width of the N,S-CDs appeared are larger than those of N-CDs. Comparing with N-CDs, the disorder degree of N,S-CDs is enhanced. It is probably attributed to rich active sites on the surface of double-doped CDs induced by introduction of S element.[29] The TEM images are shown in Figs. 1(b) and 1(c). The average diameter is about 3.7 nm for N-CDs and 3.9 nm for N,S-CDs, respectively. These particles are dispersed uniformly without obvious agglomeration. The value of interplanar spacing is 0.32 nm for N-CDs and 0.28 nm for N,S-CDs respectively, which is in accordance with the (002) diffraction plane of graphene.[30] In virtue of the existence of surface states introduced by the S-doped element, the values of them are different.[31]

In order to investigate the functional groups, FTIR measurements were conducted and shown in Fig. 2(a). The two CDs emerge similar bands centered at 1600 cm^{-1} and 3450 cm^{-1}, corresponding to the stretching vibration of the C=C/C=N and O–H/N–H, respectively. These hydrophilic groups give CDs superior hydrophilicity. The absorption peaks at 1394 cm^{-1} and 1200 cm^{-1} represent the stretching vibration of C–N. These results indicate that nitrogen atoms exist not only as amide bands on the CDs surfaces but also

as polyaromatic structure in the cores, suggesting the formation of molecular fluorophore IPCA.[32] In addition, N,S-CDs have two additional absorption peaks at 1410 cm^{-1} and 610 cm^{-1} in the spectrum, corresponding to the stretching vibration of C–S, confirming the presence of S-containing groups. More importantly, the peak intensity of N,S-CDs is increased at the low wavenumbers, especially in the C–N band. The pronounced features reflect that the addition of S promotes the formation of N-containing functional groups, resulting in more IPCA.

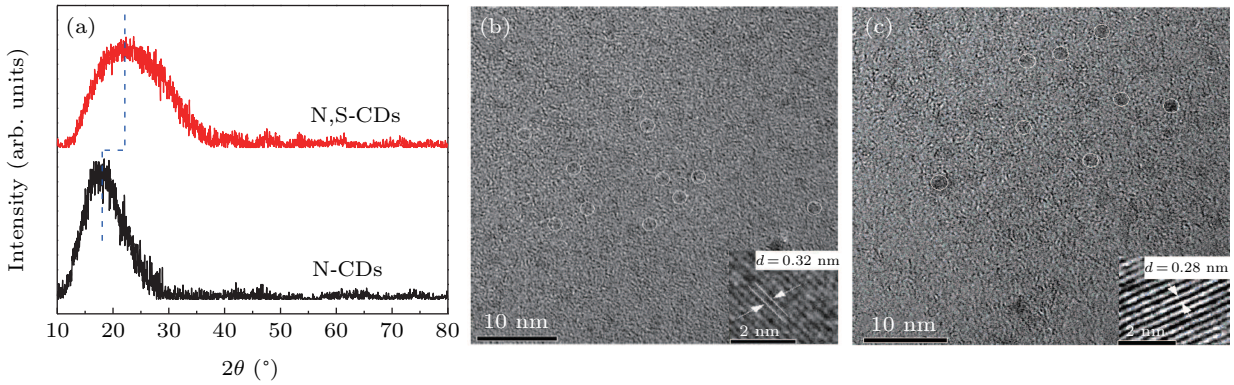


Fig. 1. (a) XRD patterns of N-CDs and N,S-CDs, TEM, and HRTEM (inset) images of N-CDs (b) and N,S-CDs (c).

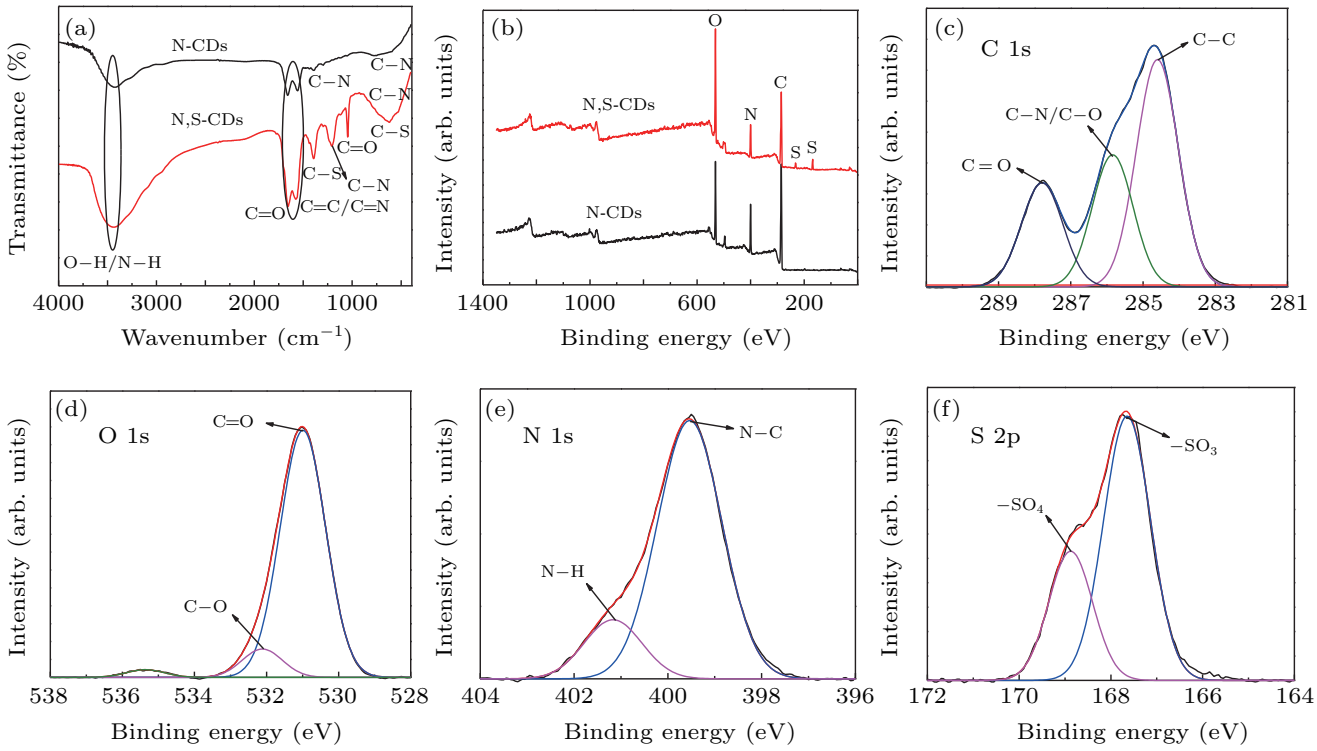


Fig. 2. (a) The FTIR spectra of N-CDs and N,S-CDs, (b) XPS spectra of N-CDs and N, S-CDs, (c)–(f) high-resolution XPS data of C 1s, O 1s, N 1s, and S 2p of N,S-CDs.

The surface chemical structure was analyzed by XPS. Both of CDs possess three distinct peaks at 284.7, 531.1, and 399.7 eV in Fig. 2(b), which present the C 1s, O 1s, and N 1s signals, respectively. For N,S-CDs, addition peak at 167.7 eV is observed, which is related to presence of S groups and further confirms the introduction of S atom into CDs. The composition of 68.5% C, 15.7% O, and 15.8% N are obtained in N-CDs, whereas the atomic percentage of C, O, N, and S are 47.6%, 33.4%, 14.5%, and 4.5% in N,S-CDs respectively. The ratio of carbon to nitrogen was expressed, *i.e.*, 68.5:15.8 for N-CDs and 47.6:14.5 for N,S-CDs, implying that the introduction of S element increases the nitrogen content in CDs, which is in agreement with FTIR results. Figures 2(c)–2(f) show the high-resolution spectra for N,S-CDs. The C 1s spectrum (Fig. 2(c)) exhibits three characteristics peaks, containing aromatic conjugated sp^2 C (C–C) at 284.59 eV, sp^3C (C–N, C–O) at 285.82 eV, and C=O/C=N at 287.79 eV. Figure 2(d) displays the O 1s high resolution spectra. There are two peaks at 531.0 eV and 532.0 eV, corresponding to C=O and C–O, respectively. The N 1s band can be deconvoluted into two

peaks at 399.7 eV (C–N–C), and 401.0 eV (N–H), which are distributed to pyridinic N and pyrrolic N, respectively. These obvious signals may originate from the molecular structure of IPCA.[23] The S 2p spectrum (Fig. 2(f)) displays two peaks at 167.6 eV and 168.9 eV, which represents sulfur existence in two states of $-SO_3$ and the $-SO_4$ respectively. The functional groups introduced by S are mainly connected to the surface states.[2,3,33] Combined with the results of FTIR and XPS results, the molecular fluorophore have been formed in the CA-based CDs, and S-containing groups have been successfully introduced on the CDs surfaces. Furthermore, the introduction of sulfur atoms can promote the formation of molecular fluorophores in the present study.

3.2. Optical characterization

The optical properties of N-CDs and N,S-CDs are compared in Fig. 3, and the absorption and fluorescence spectra are expressed. Two kinds of CDs show the absorption peaks at 240 nm and 345 nm (seen in Fig. 3(a)), which are similar to the molecular fluorophores of IPCA.[23] The results tend to ascribe the strong absorption peak at 240 nm to the π–π* transition of aromatic conjugated system sp^2 domains. The shoulder absorption peak at 345 nm might originate from the n–π* transition of C=O band. In addition, the peak of N,S-CDs at 345 nm is slightly wider than that of N-CDs, indicating that

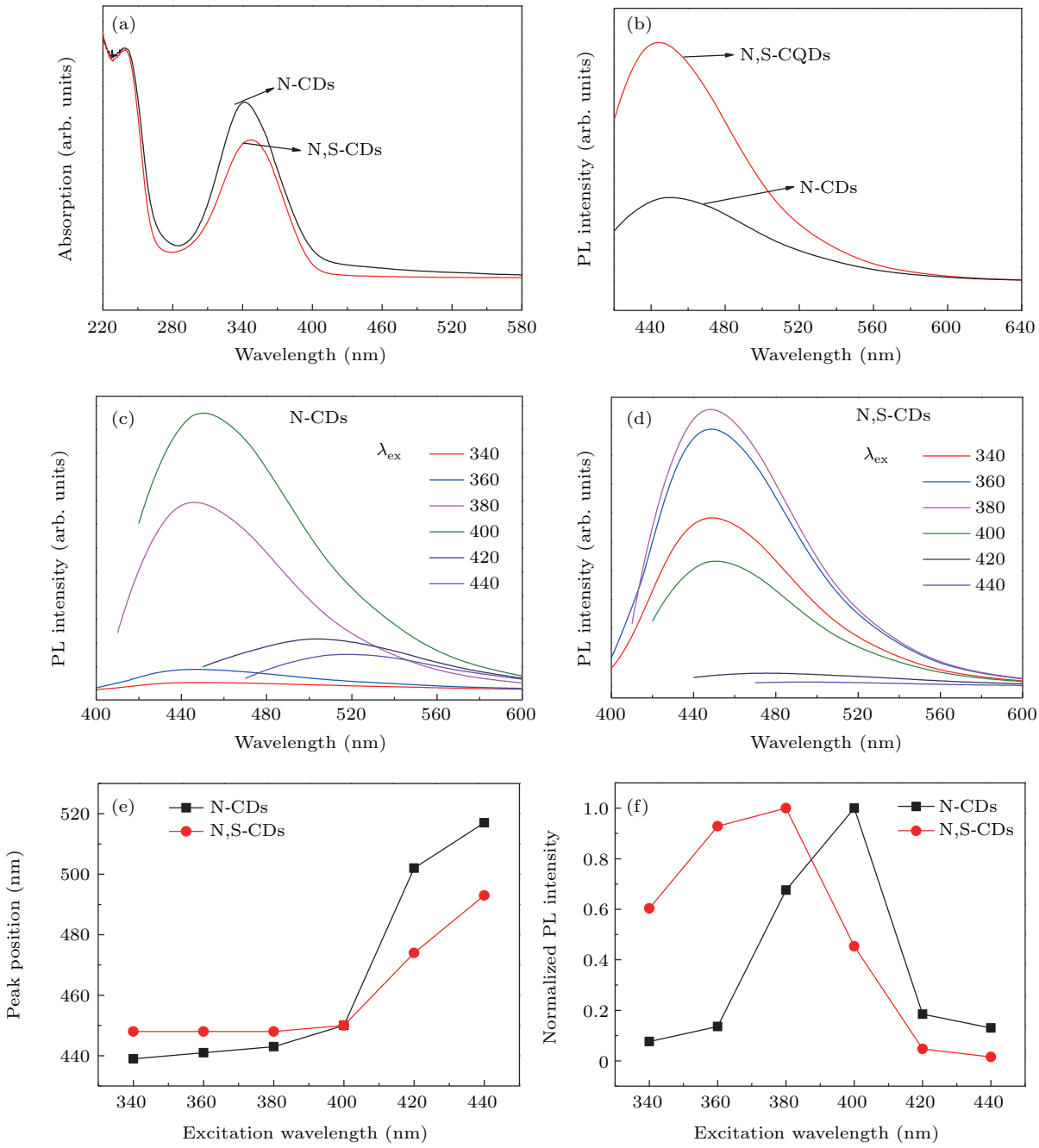


Fig. 3. (a) UV–vis absorption spectra, (b) fluorescence spectra (λ_{ex} = 380 nm) of N-CDs and N,S-CDs dispersed in water, fluorescence emission spectra of (c) N-CDs, (d) N,S-CDs, (e) peak position, and (f) normalized PL intensity at different excitation wavelengths.

more functional groups and surface states are generated due to the introduction of S element. Figure 3(b) displays the fluorescence emission spectra at 380-nm excitation. The emission peak is about 445 nm of N-CDs, which is in accordance with the emission of IPCA. The emission peak of N,S-CDs is at 439 nm, which is slightly blue shifted. The CDs after S-doping would form new functional groups on the surface, which might lead to local deformation on the CDs and induced the new energy levels.[17,34,35] As a result, the emission peak position is shifted. N,S-CDs present more blue emission than N-CDs (Fig. 3(b)), and the PLQY is up to 63.4%, which is much higher than that of N-CDs (56.4%). Undoubtedly, the sulfur doping enhances the fluorescence emission. According to the FTIR and XPS results, sulfur doping can increase the nitrogen doping and induce S-containing surface states, meaning that more C–N, C=N/C=O and new C–S bonds are produced. The newly introuduced groups are obviously responsible for the raising blue emission.[36] The PLQY of N,S-CDs is improved owing to their synergistic effect.

The fluorescence emission spectra at different excitation wavelengths were assessed and shown in Figs. 3(c) and 3(d). For two kinds of CDs, the PL emission exhibits clearly two separate regions. Under short wavelength excitation in the range of 340 nm–400 nm, the excitation-independent emission is observed, meaning that a single emissive transition is dominant. Excitation in the range of 400 nm–440 nm leads to a typical excitation-dependent emission, which comes from the newly introduced surface states.[37,38] Figures 3(e) and 3(f) show the peak position and normalized PL intensity at different excitation wavelengths. Owing to the introduction of sulfur atoms, the optimal excitation wavelength changes from 400 nm of N-CDs to 380 nm of N,S-CDs, which is more close to that of pure IPCA. The fluorescence decay curves of the two CDs were exhibited in Fig. 4. The PL lifetime of N-CDs is 11.5 ns, which is similar with that of IPCA reported by Schneider.[39] For the double doped CDs, the PL lifetime is elongated to 15.7 ns. The introduction of S element gives additional surface states to the CDs.[40] As a result, the PL lifetime is prolonged.

To further investigate the influence of S injection on molecular fluorophores, the samples with different precursor ratios were prepared. Figure 5 displays the fluorescence emission spectra of these CDs by excitation at 380 nm. For three samples that the ratio of CA:EDA:Na_2SO_3 is 1:1:1, 1:2:1, and 1:3:1, following the increase of EDA, the fluorescence intensity of CDs first increases, reaches the maximum at 1:2:1, and then decreases. Appropriate introduction of N element can increase the information of IPCA and then improve the emission, which is consistent with the reported results by Kokorina *et al.*[41] For the samples with different Na_2SO_3 ratio,

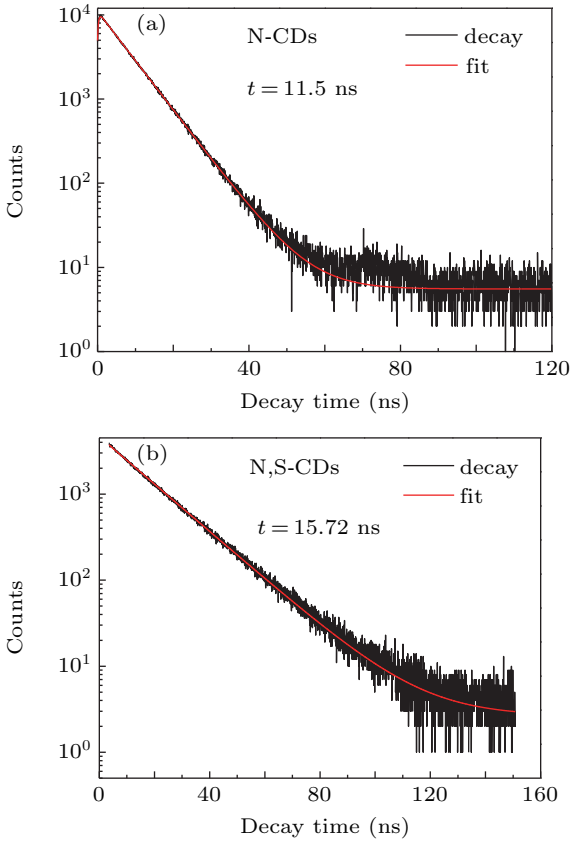


Fig. 4. Time-resolved fluorescence decay curves for N-CDs and N,S-CDs (445-nm emission under 380-nm excitation).

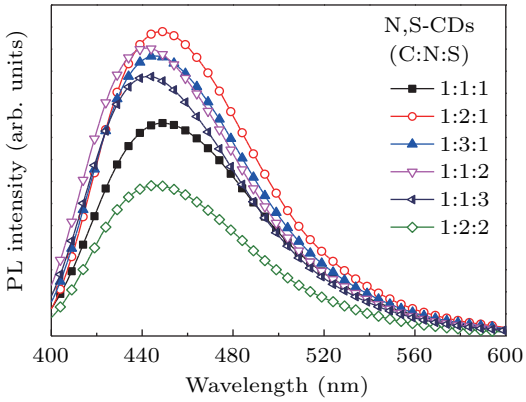


Fig. 5. The fluorescence spectra of N,S-CDs prepared with various CA:EDA:Na_2SO_3 ratios.

namely, CA:EDA:Na_2SO_3 1:1:1, 1:1:2, and 1:1:3, the optimal emission is obtained at 1:1:2 ratio. Appropriate increasing the ratio of EDA (1:2:1) or Na_2SO_3 (1:1:2) can enhance the fluorescence emission of the CDs. However, the CDs prepared with CA:EDA:Na_2SO_3 =1:2:2 exhibit the minimum emission, meaning that increasing both the ratio of EDA and Na_2SO_3 would harm the emission. Schneider *et al.*[39] suggested that fluorescence of CDs synthesized from CA and EDA mainly originates from IPCA, which may be bond to the CDs. The surface states induced by S doping are attached to the CDs surfaces. Excessive addition of the two precursors would cause the competition between the two kinds of functional groups

on the CDs surfaces, leading to the decrease of effective functional groups that can produce luminescence.[41,42] The CDs with CA:EDA:Na_2SO_3 at 1:2:1 ratio exhibit maximum fluorescence emission and minimum half-height width in the present study. The precursor ratio has little impact on the emission peak position of N,S-CDs. These results suggest that the fluorescence of N,S-CDs are decided by synergistic effect of nitrogen containing fluorophores (IPCA) and sulfur containing surface states.

3.3. Fluorescence sensitivity

The fluorescence sensitivity of the present N,S-CDs under various conditions has also been studied. Figure 6(a) presents the fluorescence spectrum under various pH conditions. The bright blue light is observed from the N,S-CDs and the fluorescence emission intensity is influenced by the solution conditions. As the pH value increases, the emission intensity increases, reaches the maximum at pH = 7, and then decreases. The neutral conditions favor the fluorescence emission of CDs, whereas strong acid or strong alkaline conditions lead to fluorescence quenching. With increasing pH value, the fluorescence emission peak shifts from 457 nm to 444 nm.

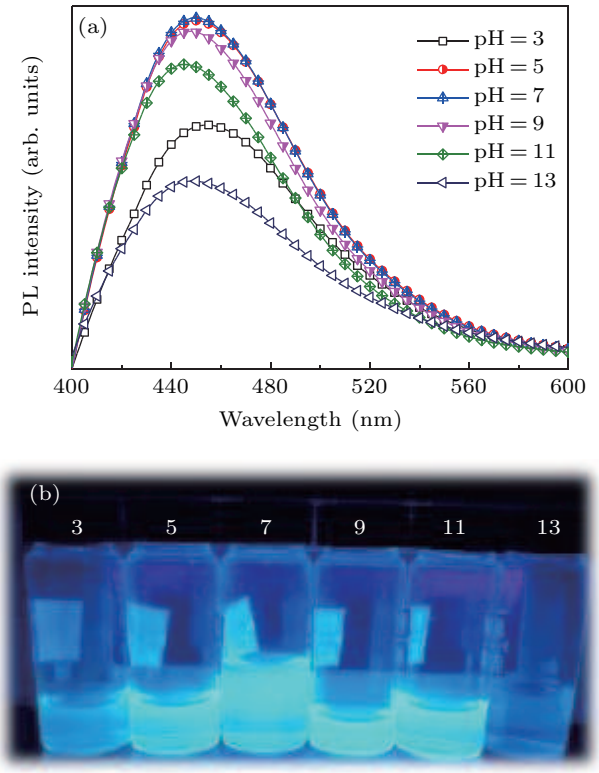


Fig. 6. (a) Fluorescence emission spectrum and (b) optical photographs of N, S-CDs in various pH conditions.

Figure 6(b) shows the optical photographs of the samples under UV irradiation at different pH conditions. The pH sensitivity of N,S-CDs is attributed to the presence of a large number of carboxyl and N–H groups. These groups give the CDs the similar structure of amino acids, which possesses various isoelectric points and dissociation constants.[9,30] As a result, the fluorescence emission occurs the changes in different pH values.

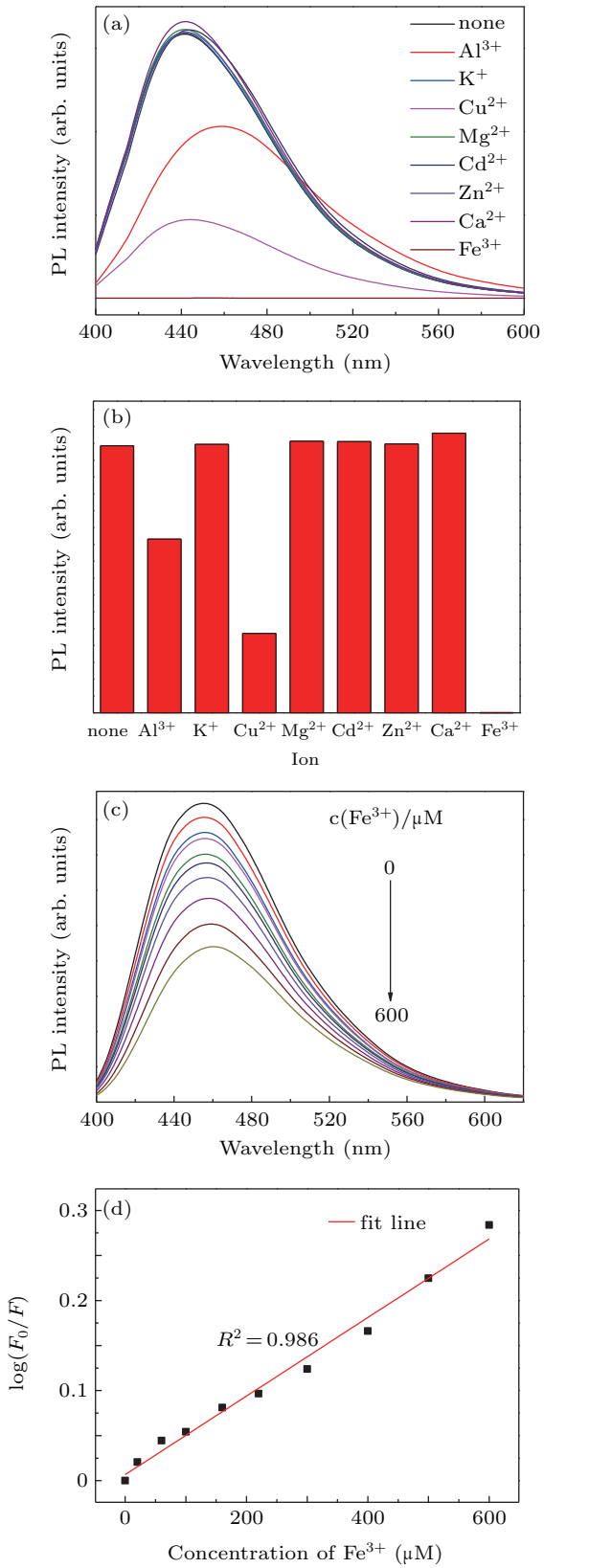


Fig. 7. (a) Fluorescence spectra, (b) comparison of fluorescence intensities of N,S-CDs after adding different metal ions, (c) fluorescence spectra of the N,S-CDs mixed with various concentrations of Fe^{3+} ions: 0, 20, 60, 100, 160, 220, 300, 400, 500, and 600 μM, (d) logarithmic relative PL intensity *versus* concentration of Fe^{3+} ions.

The fluorescence detection of the N,S-CDs were measured under the condition of various metal ions. As shown in Figs. 7(a) and 7(b), for K^+, Mg^{2+}, Cd^{2+}, Ca^{2+}, and Zn^{2+} ions, the fluorescence intensity remains almost unchanged. The obvious fluorescence quenching can be caught in the solution of Al^{3+} and Cu^{2+}ions, but the strongest quenching is found in the presence of iron ions. The quenching effect is possible contribute to the strong interaction between metal ions and functional groups attached to the CDs surfaces, which leads to form complexes and the photoelectrons migration from CDs to the metal irons, especially Fe^{3+} irons.[7,11] Figure 7(c) displays the fluorescence spectra of N,S-CDs solution added different concentrations of Fe^{3+} ions under 360-nm excitation. With the increase of Fe^{3+} concentration, the fluorescence intensity decreased gradually. Moreover, the intrinsic fluorescence peak of N,S-CDs occurs red-shift, which is due to the formation of complex between Fe^{3+} ion and CDs, just as reported by Wu *et al.*[27] The quenching efficiency (F_0/F_1) exhibits a close linearity correlation with the Fe^{3+} concentration in a range of 0 μM–600 μM, and a correlation coefficient (R^2) was calculated to be 0.986 from Fig. 7(d). The concentration of Fe^{3+} can be calculated from the following calibration equation:

$$\log(F_0/F) = -0.00254 + 3.8199 \times 10^{-4} C, \quad (1)$$

where F and F_0 are the fluorescence intensity of N,S-CDs in the addition and un-addition of metal ions, respectively, and C denotes the concentration of Fe^{3+}. The limit of detection is evaluated to be 3.31 μM at an N/S value of 3.[43,44] The results suggest that N,S-CDs can accurately detect the concentration of Fe^{3+} ions on the basis of the luminescence in a narrow range.

4. Conclusion

Citric acid-based carbon dots with modification via ethylenediamine and sodium sulfite are prepared under hydrothermal conditions in this paper. The influence of the S doping on the structural and optical characteristics, and fluorescence sensitivity of CDs has been carefully investigated. In the N,S-CDs or N-CDs, the molecular fluorophore IPCA is formed. The introduction of the S element can further promote the formation of the IPCA, and produce the additional surface states containing sulfur. According to the fluorescence lifetime measurement, the S doping increases the lifetime of CDs. The synergistic effect in critic acid-based CDs improves the fluorescence performance due to the co-doping of nitrogen and sulfur, and the photoluminescence quantum yields are increased from 56.4% for N-CDs to 63.4% for N,S-CDs. Fluorescence sensitivity results indicate that the N,S-CDs have potential applications prospect in strong alkaline solution and Fe^{3+} ion detections. Introducing independent sulfur source is a practicable method to investigate the influence factors of molecular fluorophores in CDs.

References

[1] Shen J, Zhang T, Cai Y, Chen X, Shang S and Li J 2017 *New J. Chem.* **41** 11125
[2] Quan Z Q, Xu Y H, Liu M L, Cui L and Liu J Q 2016 *Carbon* **104** 169
[3] Zhan H and Gu Y 2018 *Chin. Phys. B* **27** 038103
[4] Yuan B, Guan S, Sun X, Li X, Zeng H, Xie Z, Chen P and Zhou S 2018 *ACS Appl. Mater. Interfaces* **10** 16005
[5] Yuan F, Wang Z, Li X, Li Y, Tan Z A, Fan L and Yang S 2017 *Adv. Mater.* **29** 1604436
[6] Zhu Z J, Li Q X, Li P, Xun X J, Zheng L Y, Ning D D and Su M 2019 *PLoS ONE* **14** e0216230
[7] Wu H, Jiang J, Gu X and Tong C 2017 *Microchim. Acta* **184** 2291
[8] Luo H, Papaioannou N, Salvadori E, Roessler M M, Ploenes G, van Eck E R, Tanase L C, Feng J, Sun Y and Yang Y 2019 *Chem. Sus. Chem.* **12** 4432
[9] Sun D, Ban R, Zhang P H, Wu G H, Zhang J R and Zhu J J 2013 *Carbon* **64** 424
[10] Ma Z, Ming H, Huang H, Liu Y and Kang Z 2012 *New J. Chem.* **36** 861
[11] Qi H J, Teng M, Liu M, Liu S X, Li J, Yu H P, Teng C B, Huang Z H, Liu H, Shao Q, Umar A, Ding T, Gao Q and Guo Z H 2019 *J. Colloid Interface Sci.* **539** 332
[12] Barman M K, Jana B, Bhattacharyya S and Patra A 2014 *J. Phys. Chem. C* **118** 20034
[13] Gong K, Du F, Xia Z, Durstock M and Dai L 2009 *Science* **323** 760
[14] Wang L, Yin Y, Jain A and Zhou H S 2014 *Langmuir* **30** 14270
[15] Gu D, Zhang P, Zhang L, Liu H, Pu Z and Shang S 2018 *Opt. Mater.* **83** 272
[16] Ye Q H, Yan F Y, Shi D C, Zheng T C, Wang Y Y, Zhou X G and Chen L 2016 *J. Photoch. Photobio. B* **162** 1
[17] Li F, Liu C, Yang J, Wang Z, Liu W and Tian F 2013 *RSC Adv.* **4** 3201
[18] Dhenadhayalan N, Lin K C, Suresh R and Ramamurthy P 2016 *J. Phys. Chem. C* **120** 1252
[19] Zhang W K, Liu Y Q, Meng X R, Xu H, Xu Y Q, Liu B Y, Fang X M, Li H B and Ding T 2017 *RSC Adv.* **7** 20345
[20] Krysmann MJ, Kelarakis A, Dallas P and Giannelis E P 2012 *J. Am. Chem. Soc.* **134** 747
[21] Li X, Zhang S, Kulinich S A, Liu Y and Zeng H 2014 *Sci. Rep.* **4** 4976
[22] Zhai X, Zhang P, Liu C, Bai T, Li W, Dai L and Liu W 2012 *Chem. Commun.* **48** 7955
[23] Song Y, Zhu S, Zhang S, Fu Y, Wang L, Zhao X and Yang B 2015 *J. Mater. Chem. C* **3** 5976
[24] Kasprzyk W, Bednarz S, Zmudzki P, Galica M and Bogdal D 2015 *RSC Adv.* **5** 34795
[25] Zhang Y and He J H 2015 *Phys. Chem. Chem. Phys.* **17** 20154
[26] Gao F, Ma S Y, Li J, Dai K, Xiao X C, Zhao D and Gong W F 2017 *Carbon* **112** 131
[27] Wu H F, Jiang J H, Gu X T and Tong C L 2017 *Microchim. Acta* **184** 2291
[28] Wang H Y, Lu Q J, Hou Y X, Liu Y L and Zhang Y Y 2016 *Talanta* **155** 62
[29] Li Y, Hu Y, Zhao Y, Shi G Q, Deng L E, Hou Y B and Qu L T 2011 *Adv. Mater.* **23** 776
[30] Meierhofer F, Dissinger F, Weigert F, Jungclaus J, Müller-Caspary K, Waldvogel S R, Resch-Genger U and Voss T 2020 *J. Phys. Chem. C* **124** 8894
[31] Dong Y, Pang H, Yang H B, Guo C, Shao J, Chi Y, Li C M and Yu T 2013 *Angew. Chem. Int. Ed.* **52** 7800
[32] Ding H, Wei J S and Xiong H M 2014 *Nanoscale* **6** 13817

[33] Xia W, Wang Y, Bergsträßer R, Kundu S and Muhler M 2007 *Appl. Surf. Sci.* **254** 247

[34] Zhu S J, Song Y B, Zhao X H, Shao J R, Zhang J H and Yang B 2015 *Nano Research* **8** 355

[35] Bao L, Zhang Z L, Tian Z Q, Zhang L, Liu C, Lin Y, Qi B P and Pang D W 2011 *Adv. Mater.* **23** 5801

[36] Xu Y, Wu M, Liu Y, Feng X Z, Yin X B, He X W and Zhang Y K 2013 *Chem. Eur. J* **19** 2276

[37] Ye Y, Yang D, Chen H, Guo S, Yang Q, Chen L, Zhao H and Wang L 2020 *J Hazard. Mater.* **381** 121019

[38] LeCroy G E, Messina F, Sciortino A, Bunker C E, Wang P, Shiral Fernando K A and Sun Y P 2017 *J. Phys. Chem. C.* **121** 28180

[39] Schneider J, Reckmeier C J, Xiong Y, von Seckendorff M, Susha A S, Kasaák P and Rogach A L 2017 *J. Phys. Chem. C* **121** 2014

[40] Liu M L, Chen B B, Li C M and Huang C Z 2019 *Green Chemi.* **21** 449

[41] Kokorina A A, Bakal A A, Shpuntova D V, Kostritskiy A Y, Beloglazova N V, Saeger S D, Sukhorukov G B, Sapelkin A V and Goryacheva Y I 2019 *Sci. Rep.* **9** 14665

[42] Dang T H T, Mai V T, Le Q T, Duong N H and Mai X D 2019 *Chem. Phys.* **527** 110503

[43] Zou S, Hou C, Fa H, Zhang L, Ma Y, Dong L, Li D, Huo D and Yang M 2017 *Sensor. Actuat. B* **239** 1033

[44] Li H Y, Xu Y, Zhao L, Ding J, Chen M Y, Chen G R, Li Y and Ding L 2019 *Carbon* **143** 391